Study on Coupling Characteristics of Electromagnetic Wave Penetrating Metallic Enclosure with Rectangular Aperture

Gang Wu, Zhi-Qiang Song, Xin-Gang Zhang, and Bo Liu

Xi'an division of China Academy of Space Technology
Xi'an 710100, Shaanxi, P. R. China
woogung@126.com, 17151320@qq.com, xinkou224@126.com, CAST504@yeah.net

Abstract ― The coupling characteristics of the electromagnetic wave penetrating the metallic enclosure with a rectangular aperture are studied using the hybrid approach which applies the mode-matching technique and the mixed potential integral equation based on the method of moments. The aperture thickness, the polarization direction of incident wave, and high-order modes are all considered in the simulation. The calculated electric field at the centre of the enclosure is compared with data obtained by measurement and other numerical techniques to validate the accuracy and the efficiency of the proposed approach. The electric field distributions inside the metallic enclosure are also presented. Furthermore, this approach is extended to account for the effects of narrow aperture thicknesses and polarization directions. The results demonstrate that the electric field is enhanced around the aperture at the resonant frequency and the coupling electric field amplitude at the center point of the enclosure is also higher than that in the ambient area. It is also noted that the variation of the narrow aperture thicknesses and the different polarization directions act on the coupling characteristics significantly.

Index Terms ― Electric field distribution, electromagnetic coupling, mixed potential integral equation, mode matching, resonance.

I. INTRODUCTION

Electromagnetic shielding by the aid of metallic enclosures is frequently used to reduce emissions from electromagnetic interferences (EMI). At the same time, apertures perforated in the enclosure will compromise its shielding effectiveness. In order to take some measures to limit the influence of the interference energy, it is extremely important to analyze the coupling characteristics of the electromagnetic wave penetrating the metallic enclosures with apertures.

The electromagnetic coupling characteristics can be analyzed using numerical or analytical methods. Numerical methods, such as the finite difference time domain (FDTD) method [1-7], the method of moments (MoM) [8-11], the finite element method (FEM) [12], and the hybrid methods [13-14], can model enclosures with sufficient detail but often requires large computing time and memory, and the analytical approaches based on various simplifying assumptions [15-16] are also subject to many severe limitations even though providing a much faster means.

This paper presents a rigorous full-wave solution which combines the mode-matching technique and the mixed potential integral equation based on MOM to study the coupling characteristics of electromagnetic wave penetrating a metallic enclosure with a rectangular aperture. Some influencing factors, such as the aperture thickness, the polarization direction of the incident wave and high-order modes, are considered in the numerical simulation. Finally, the simulation results are compared with data obtained by measurement and other numerical techniques thus showing the accuracy and the efficiency of the proposed approach.

Submitted On: May 23, 2011
Accepted On: August 24, 2011

II. MATHEMATICAL FORMULATION

A metallic enclosure with dimensions $a \times b \times h$ (inner face) illuminated by the electromagnetic wave is shown in Figure 1, having a rectangular aperture with dimensions $w \times l$ in the front wall. The walls whose thicknesses are t are assumed to be perfectly conducting.

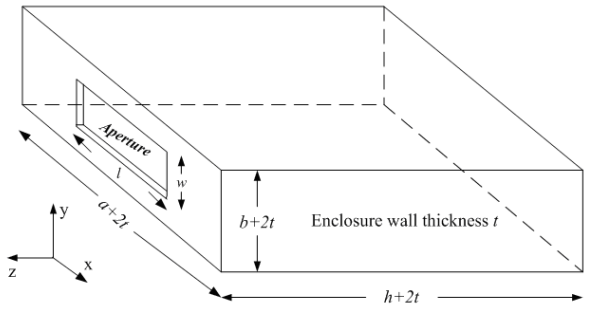

Fig. 1. Geometry of the rectangular enclosure with aperture.

As shown in Figure 2, the entire equivalent model of EMI coupling into a rectangular enclosure through a non-zero thickness aperture can be separated into two sub-problems by employing Schelkunoff's field equivalent principle: the interior problem and the exterior problem. The interior problem is composed of region I and region II which can be regarded as the rectangular waveguides, while the exterior problem is considered as a half free space (region III) with an equivalent magnetic current and an incident electromagnetic wave. It should be noted that the plane z=t where the aperture is perforated is regarded as an infinite conductive plane [17].

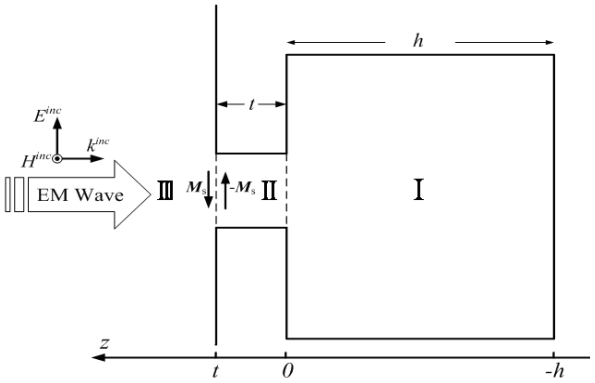

Fig. 2. Equivalent model for aperture replaced by magnetic current.

A. Interior problem

From Maxwell's equations, the tangential electric field and the tangential magnetic field in the waveguides can be represented by

$$\boldsymbol{E}_t = -\frac{j\omega\mu}{k_c^2}\nabla_t H_z \times \boldsymbol{z} + \frac{1}{k_c^2}\nabla_t \frac{\partial E_z}{\partial z} \quad , \tag{1}$$

$$\boldsymbol{H}_t = \frac{j\omega\varepsilon}{k_c^2}\nabla_t E_z \times \boldsymbol{z} + \frac{1}{k_c^2}\nabla_t \frac{\partial H_z}{\partial z} \quad . \tag{2}$$

In order to solve Maxwell's equations conveniently, the electric and the magnetic vector potentials are introduced whose z-direction components are A_{ez} and A_{hz}, respectively. Then z-direction components of the electric field and the magnetic field are given by

$$E_z = \frac{k_c^2}{j\omega\varepsilon} A_{ez} \quad , \tag{3}$$

$$H_z = \frac{k_c^2}{j\omega\mu} A_{hz} \quad . \tag{4}$$

Region I and Region II can be regarded as the rectangular waveguides, the aperture waveguide-to-rectangular enclosure junction can be modeled by the mode-matching technique. And then substituting (3) and (4) into (1) and (2), the tangential electromagnetic fields in Region i (i=I,II) can be expressed as follows [18]:

$$\boldsymbol{E}_t^i = -\nabla_t A_{hz}^i \times \boldsymbol{z} + \frac{1}{j\omega\varepsilon}\nabla_t \frac{\partial A_{ez}^i}{\partial z} \tag{5}$$

$$\boldsymbol{H}_t^i = \nabla_t A_{ez}^i \times \boldsymbol{z} + \frac{1}{j\omega\mu}\nabla_t \frac{\partial A_{hz}^i}{\partial z} \tag{6}$$

$$A_{hz}^i(x,y,z) = \sum_{q=1}^{N} Q_{hq}^i T_{hq}^i \left[A_{hq}^{i+} e^{-\Gamma_{hq}^i z} + A_{hq}^{i-} e^{\Gamma_{hq}^i z} \right] \tag{7}$$

$$A_{ez}^i(x,y,z) = \sum_{q=1}^{N} Q_{eq}^i T_{eq}^i \left[A_{eq}^{i+} e^{-\Gamma_{eq}^i z} - A_{eq}^{-} e^{\Gamma_{eq}^i z} \right], \tag{8}$$

where ε is permittivity of free space and μ is magnetic permeability of free space, T_e and T_h is the eigenfunction of the TM (e) and TE (h) modes, respectively. In the same way, A_e and A_h □are the modal amplitude coefficients, □e and □h are the propagation constants, Q_e and Q_h are the normalized factors such that the power carried by each mode is 1 Watt. q is the mode index.

On the assumption that there are N TM modes and N TE modes propagating in the waveguides, the $2N \times 1$ modal amplitude coefficients matrix of the positive and negative z-direction modes in the

waveguide Region i, $\boldsymbol{A}^{i+}$ and $\boldsymbol{A}^{i-}$ can be described as:

$$A^{i+}=\begin{bmatrix}A_e^{i+}\\A_h^{i+}\end{bmatrix}\qquad A^{i-}=\begin{bmatrix}A_e^{i-}\\A_h^{i-}\end{bmatrix}\ . \tag{9}$$

In terms of the tangential electric field and the tangential magnetic field components matching at the boundary between Region I and Region II, respectively, the coupling matrix $\boldsymbol{M}$ whose size is $2N\times 2N$ is obtained [19]. Therefore, the relationship between the modal amplitude coefficients in Region I and II can be expressed as:

$$A^{I+}+A^{I-}=M\left(A^{II+}+A^{II-}\right)\ , \tag{10}$$

$$M^T\left(A^{I+}-A^{I-}\right)=A^{II+}-A^{II-}\ . \tag{11}$$

On account of the region I is considered as an end-shorted waveguide, what can be obtained is written as:

$$A^{I+}=-L^I A^{I-} \tag{12}$$

where $L^I=diag\left\{e^{-2\Gamma_j^I h}\right\},\ j=e,h$.

Substituting (12) into (10) and (11) gives a matrix equation describing the relationship of the modal amplitude coefficients in Region II:

$$A^{II+}=\rho A^{II-} \tag{13}$$

where $\rho=(U+P)^{-1}(U-P)$

$$P=M^T\left(L^I+U\right)\left(U-L^I\right)^{-1}M\ .$$

U is the $2N\times 2N$ unit matrix.

Substituting (12) and (13) into (10) and (11) gives a matrix equation:

$$A^{I-}=\left(U-L^I\right)^{-1}M\left(\rho+U\right)A^{II-}\ . \tag{14}$$

B. Exterior problem

According to the equivalence principle, the aperture on the plane z=t can be replaced by the equivalent surface magnetic current $\mathbf{M}_s$ as shown in Figure 2, given by

$$\boldsymbol{M}_s=-\boldsymbol{n}\times\boldsymbol{E}_t^{II}(t)\ , \tag{15}$$

with $\boldsymbol{n}$ being the normal unit vector pointing outwards.

By means of image theory, the equivalent magnetic current $2\mathbf{M}_s$ substitutes as the equivalent source for the half-space. Mathematically, the magnetic field $\mathbf{H}^{Ms}$ due to $2\mathbf{M}_s$ in Region III can be written as follows [20]:

$$\boldsymbol{H}^{M_S}=-j\omega\boldsymbol{F}(\boldsymbol{r})-\nabla\phi_m(\boldsymbol{r})\ . \tag{16}$$

To simplify the notation, the inner product can be defined:

$$\langle A,B\rangle=\iint_{sa}A\cdot B dS\ , \tag{17}$$

where the integration extends over the aperture on the plane z=t for the 2D case. Then, the electric vector potential **F** and the magnetic scalar potential ϕ_m at a field point **r** are obtained [21]:

$$\boldsymbol{F}(\boldsymbol{r})=2\varepsilon\left\langle\boldsymbol{M}_s(\boldsymbol{r}'),\bar{\bar{\boldsymbol{G}}}_{free}^{F}(\boldsymbol{r}\,|\,\boldsymbol{r}')\right\rangle\ , \tag{18}$$

$$\phi_m(\boldsymbol{r})=\frac{2j}{\omega\mu}\left\langle\nabla_t'\cdot\boldsymbol{M}_s(\boldsymbol{r}'),G_{free}^{\phi_m}(\boldsymbol{r}\,|\,\boldsymbol{r}')\right\rangle\ . \tag{19}$$

$\bar{\bar{\boldsymbol{G}}}_{free}^{F}$ and $G_{free}^{\phi_m}$ are the dyadic and the scalar Green's function for the half free space respectively.

C. Final matrix equation

According to the continuity of the tangential magnetic field through the aperture on the plane z=t, the magnetic formulation can be accomplished by enforcing:

$$\boldsymbol{H}_t^{M_S}+2\boldsymbol{H}_t^{inc}=\boldsymbol{H}_t^{II}(t)\ . \tag{20}$$

The equation (20) can be solved by MoM, and then the equivalent magnetic current $\mathbf{M}_s$ is expanded by a set of vector basis functions $\mathbf{W}_n$ with unknown coefficients K_n as:

$$\boldsymbol{M}_s=\sum_{n=1}^{2N}K_n\cdot\boldsymbol{W}_n\ . \tag{21}$$

Moreover, the Galerkin procedure is applied. Setting the weighting function **W** ($2N\times 1$) equal to the basis function as:

$$\boldsymbol{W}=\begin{bmatrix}\boldsymbol{W}_e\\\boldsymbol{W}_h\end{bmatrix}=\begin{bmatrix}\dfrac{\Gamma_e^{II}}{j\omega\varepsilon}Q_e^{II}\left(\nabla_t T_e^{II}\right)\times\boldsymbol{z}\\-Q_h^{II}\left(\nabla_t T_h^{II}\right)\end{bmatrix}\ . \tag{22}$$

In terms of the orthogonality of expansion functions, the mixed potential integral equation (20) can be shown as the following matrix equation:

$$TK+I^{inc}=Z\ , \tag{23}$$

where

$$\begin{aligned}TK&=-j\omega\langle\boldsymbol{W},\boldsymbol{F}\rangle-\langle\boldsymbol{W},\nabla\phi_m\rangle\\&=-j\omega\langle\boldsymbol{W},\boldsymbol{F}\rangle+\langle\nabla_t\boldsymbol{W},\phi_m\rangle\\K&=L^{II}A^{II+}+\left(L^{II}\right)^{-1}A^{II-}\\I^{inc}&=\left\langle\boldsymbol{W},2\boldsymbol{H}_t^{inc}\right\rangle\end{aligned}$$

$$Z = \left\langle \boldsymbol{W}, \boldsymbol{H}_t^{II} \right\rangle = L^{II} A^{II+} - \left(L^{II}\right)^{-1} A^{II-}$$

$$L^{II} = diag\left\{ e^{-\Gamma_j^{II} t} \right\} \qquad j = e, h$$

It is worth noting that the matrix $\mathbf{I}^{inc}$ relates to the polarization direction of the incident wave. Furthermore, putting (20) together with (13), the unknown modal coefficients $\mathbf{A}^{II-}$ are readily obtained if the incident plane wave has been given:

$$A^{II-} = \left[\left(L^{II} \rho - (L^{II})^{-1} \right) - T \left(L^{II} \rho + (L^{II})^{-1} \right) \right]^{-1} I^{inc} \cdot \tag{24}$$

Finally, introducing (24) into the matrix equations (12) and (14), all the modes propagating in the enclosure can be calculated. The electromagnetic fields at any point in the enclosure with non-zero thickness aperture can be calculated consequently.

III. MEASUREMENT SETUPS

In the measurement setup of Figure 3, a semi anechoic chamber of 11.37m× 4.6m× 3.0m is used, where the walls are covered with absorbing cones except for the conducting floor. The log periodic antenna—TX in Figure 3— is connected via a RF amplifier to an Agilent E8157D signal generator as the source of the field. The enclosure indicated by EUT is constructed of five pieces of aluminum and one plate of aluminum for the face containing the aperture. Measurements are made by placing the R&S HZ-15 probe in the centre of the enclosure and the output is shown on an Agilent E4440A spectrum analyzer. The effect of the ground plane and the attenuation of cables are accounted for by a suitable calibration procedure.

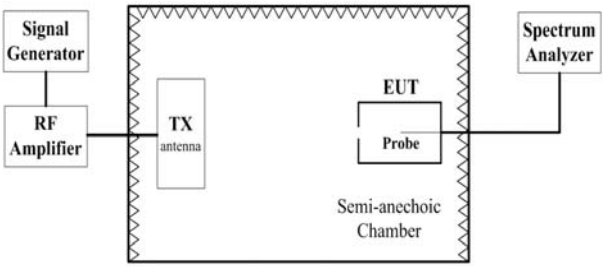

Fig. 3. Measurement setups in a semi-anechoic chamber.

IV. NUMERICAL EXAMPLES

For the analysis of electromagnetic coupling characteristics, a typical rectangular enclosure with inner dimensions 30cm×12cm×30cm is considered, having a narrow aperture of size 10cm×0.5cm with thickness t=1.5mm located at the center of the front wall. In addition, the incident wave is propagating along negative z-direction with an intensity of 377 V/m; and its polarization direction is parallel to the short edge of the aperture (y-axis), which goes by the name of vertical polarization.

A. Validation of proposed method

In this paper, the observation point is located at the center of the enclosure. For the whole model, there are 50 TM modes and 50 TE modes introduced to obtain high accuracy results.

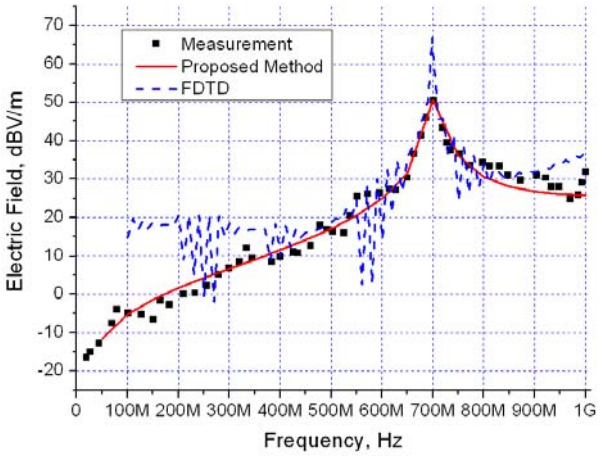

Fig. 4. Simulated and measured electric field amplitude varies with frequency at center of the enclosure.

From Figure 4, it can be seen that the results obtained by the proposed approach are in good agreement with the measurement data. The first resonant frequency 700MHz is predicted accurately at which TE_{101} mode is excited in this metallic enclosure and the coupling energy reaches its maximum over the frequency from 100MHz up to 1.0GHz. This can be very useful in optimizing the shielding devices to get some resonant frequencies filtered and minimize the EMI. In addition, the results are compared with the data obtained by FDTD. It should be mentioned that it only takes about 12 minutes and 200MByte

memory for the proposed approach to calculate the coupling electric field for 20 frequencies, while it takes 55 minutes and 350MByte memory for FDTD on the same business PC. Furthermore, taking this structure all the same, it requires more than 1 hour and 1.2GByte memory for FEM to obtain the results at 20 frequencies in [22]. This illustrates the efficiency of the proposed approach.

B. Electric field distributions inside enclosure

The metallic enclosure itself possesses a set of characteristic resonance behavior excited by external interference signals. What is more, the presence of apertures cut in the enclosure complicates resonant characteristics of the enclosure. So the electric field distributions inside the enclosure with an aperture at the resonant frequency are expected. It is useful for designers laying out the electronic components to avoid the damage caused by the external interference signals. In the following simulation figures, the incident-wave frequency is chosen to be the first resonant frequency 700 MHz, and the coupling electric field distributions inside the aforementioned enclosure are presented.

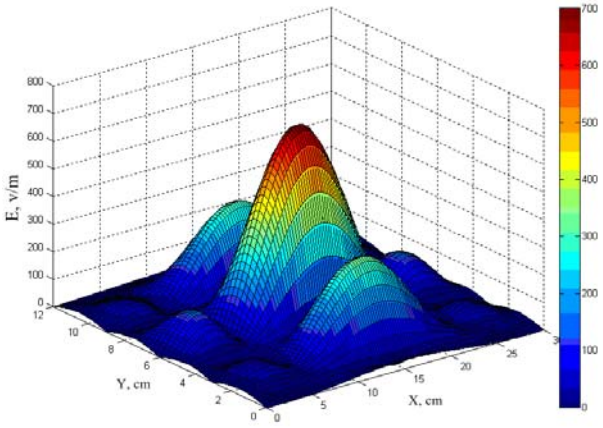

Fig. 5. Electric field distributions on the XOY plane of the enclosure at z=0cm (700MHz).

Figures 5 and 6 depict the coupling electric field distributions on the XOY plane of the enclosure at z=0cm and z=–15cm respectively. In Figure 5, it can be seen that the coupled electric field amplitude adjacent to the aperture is much higher than the incident, namely, the electric field amplitude is enhanced around the aperture. This is owing to additional enclosure-aperture interactions and the influence of high-order modes.

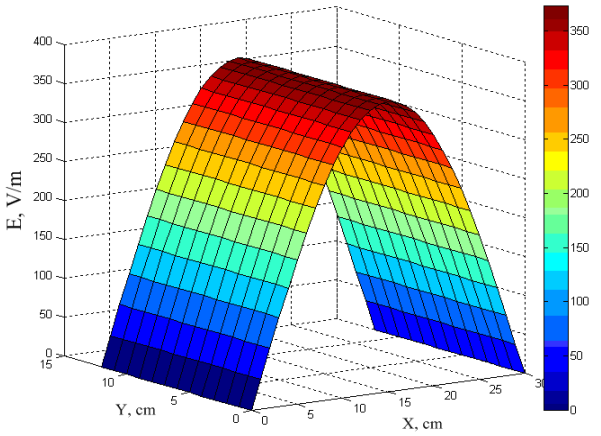

Fig. 6. Electric field distributions on the XOY plane of the enclosure at z=-15cm (700MHz).

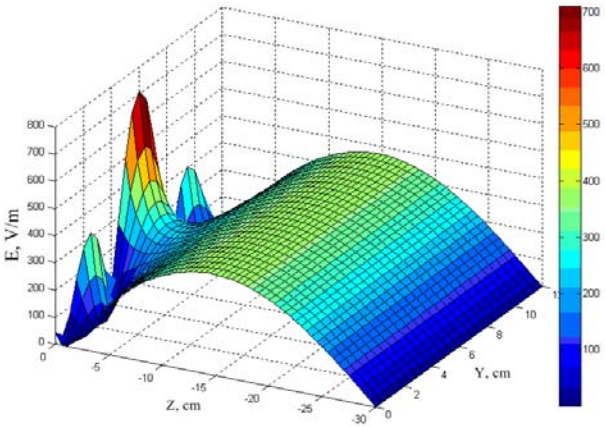

Fig. 7. Electric field distributions on the YOZ planes in the middle of the enclosure (700MHz).

The distributions of the coupled electric field on the YOZ and XOZ planes in the middle of the enclosure are shown in Figs. 7 and 8, respectively. The fact that the coupling electric field amplitude is the highest in the small area adjacent to the aperture validates the electric field amplitude being enhanced around the aperture. Furthermore, from Fig. 6 to Fig. 8, it is obvious that the coupling electric field amplitude at the center point of the enclosure is also higher than that in the ambient area.

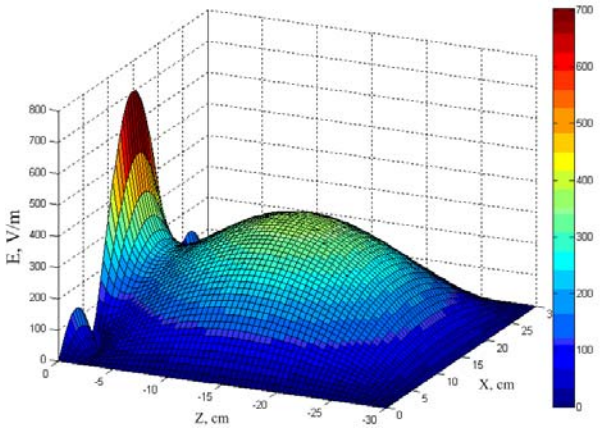

Fig. 8. Electric field distributions on the XOZ planes in the middle of the enclosure (700MHz).

C. Effect of narrow aperture thicknesses

In order to study the effect of various aperture thicknesses on coupling characteristics of electromagnetic wave penetrating a metallic enclosure through a narrow aperture, the coupling electric field at the center of the enclosure varying with the thicknesses of the aperture is considered. The narrow aperture thicknesses considered cover commonly used values: 0.5, 1.5, 3, 5, 8, and 10mm. Simulation results are displayed as a function of aperture thickness in Fig. 9. It is found that with the narrow aperture thickness increasing, the amplitude of the coupling electric field is decreasing, i.e., electromagnetic shielding of the enclosure is improved.

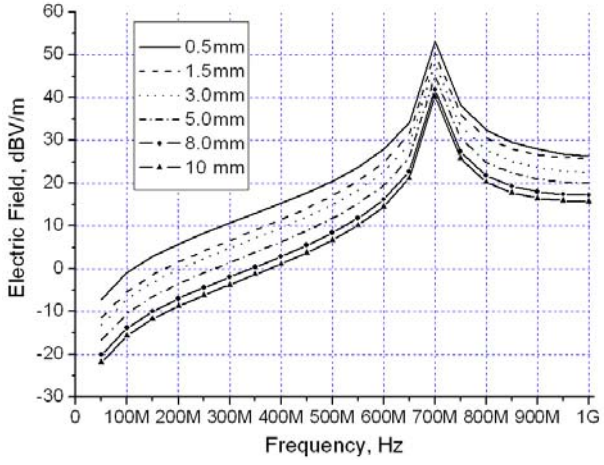

Fig. 9. Comparison of Electric fields at center of the rectangular enclosure with various narrow aperture thicknesses.

D. Effect of different polarizations

In this part, the effect of the polarization directions of the incident wave to the coupling characteristics is investigated. Compared with the vertical polarization, the horizontally polarized incident wave whose electric field polarization direction is parallel to the long edge of the aperture (x-axis) is introduced. The coupling electric field at the center of the enclosure with regard to different polarizations is shown in Fig. 10. It should be noted that the coupling electric field amplitude of the vertically polarized incident wave is higher than that of the horizontally polarized one at the center of the rectangular enclosure.

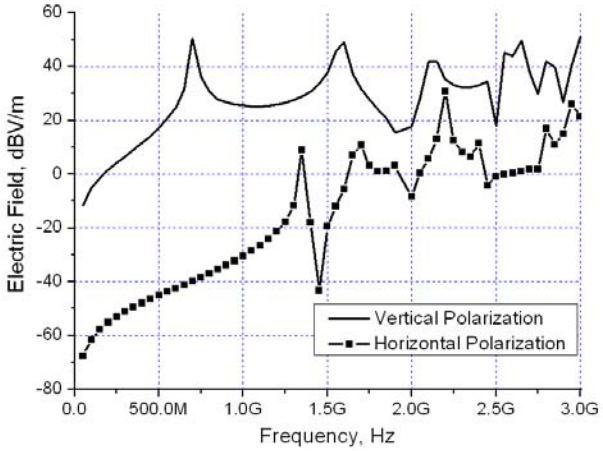

Fig. 10. Electric field at center of the rectangular enclosure with different polarizations.

V. CONCLUSIONS

The coupling characteristics of the electromagnetic wave penetrating the metallic enclosures with non-zero thickness apertures are hot issues. By matching the continuity condition of tangential electromagnetic field components across the aperture surface and the boundary between the aperture waveguide and the rectangular enclosure, the unknown modal amplitude coefficients are calculated and the electromagnetic fields inside the rectangular enclosure are determined in this paper. Usage of the proposed approach to evaluate the field distributions inside the enclosure should be helpful for laying out the vulnerable semiconductor components to limit the influence of external

electromagnetic radiation. Furthermore, the numerical simulations are directly related to the design of efficient shielding enclosures that are commonly used to protect inside components.

REFERENCES

[1] J. Z. Lei, C. H. Liang, and Y. Zhang, "Study on Shielding Effectiveness of Metallic Cavities with Apertures by Combining Parallel FDTD Method with Windowing Technique," *Progress in Electromagnetics Research*, PIER 74, pp. 85–112, 2007.

[2] J. Chen and A. Zhang, "A Subgridding Scheme Based on the FDTD Method and HIE-FDTD Method," *Applied Computational Electromagnetic Society (ACES) Journal*, vol. 26, no. 1, pp. 1–7, 2011.

[3] X. Li, J.-H. Yu, Q.-Di Wang, and Y.-M. Li, "Extension of the 2-D CP-FDTD Thin Slot Algorithm to 3-D for Shielding Analysis," *Applied Computational Electromagnetic Society (ACES) Journal*, vol. 24, no. 1, pp. 16–20, 2009.

[4] R. I. Macpherson, N. J. Ryan, R. I. Macpherson, and N. J. Ryan, "Reducing Electromagnetic Coupling in Shielded Enclosures using a Genetic Algorithm -- Finite-Difference Time-Domain Solver," *Applied Computational Electromagnetic Society (ACES) Journal*, vol. 18, no. 3, pp. 144–150, 2003.

[5] M. Li, J. Nuebel, J. L. Drewniak, R. E. DuBroff, T. H. Hubing, and T. P. Van Doren, "EMI from Airflow Aperture Arrays in Shielding Enclosures – Experiments, FDTD, and MoM Modeling," *IEEE Trans. Electromagn. Compat.*, vol. 42, no. 3, pp. 265–275, 2000.

[6] W. H. Yu, R. Mittra, and S. Chakravarty, "Stability Characteristics of Absorbing Boundary Conditions in Microwave Circuit Simulations," *IEEE Trans. Antennas Propagat.*, vol. 49, no. 9, pp. 1347–1349, 2001.

[7] N. Kantartzis and T. Tsiboukis, "A Higher-Order Non-Standard FDTD-PML Method for the Advanced Modeling of Complex EMC Problems in Generalized 3-D Curvilinear Coordinates," *IEEE Trans. Electromagn Compat.*, vol. 46, no. 1, pp. 2-11, 2004.

[8] R. Araneo and G. Lovat, "Analysis of the Shielding Effectiveness of Metallic Enclosures Excited by Internal Sources Through an Efficient Method of Moment Approach," *Applied Computational Electromagnetic Society (ACES) Journal*, vol. 25, no. 7, pp. 600–611, 2010.

[9] R. Araneo and G. Lovat, "Fast MoM Analysis of the Shielding Effectiveness of Rectangular Enclosures with Apertures, Metal Plates, and Conducting Objects," *IEEE Trans. Electromagn. Compat.*, vol. 51, no. 2, pp. 274-283, 2009.

[10] R. Araneo and G. Lovat, "An Efficient MoM Formulation for the Evaluation of the Shielding Effectiveness of Rectangular Enclosures with Thin and Thick Apertures," *IEEE Trans. Electromagn. Compat.*, vol. 50, no. 2, pp. 294-304, 2008.

[11] F. Olyslager, E. Laermans, D. De Zutter, S. Criel, R. De Smedt, N. Lietaert, and A. De Clercq, "Numerical and Experimental Study of the Shielding Effectiveness of a Metallic Enclosure," *IEEE Trans Electromagn Compat.*, vol. 41, no. 3, pp. 202-213, 1999.

[12] S. Benhassine, L. Pichon, and W. Tabbara, "An Efficient Finite-Element Time-Domain Method for the Analysis of the Coupling between Wave and Shielded Enclosure," *IEEE Trans. Magn.*, vol. 38, no. 2, pp. 709–712, 2002.

[13] C. Feng and Z. Shen, "A Hybrid FD-MoM Technique for Predicting Shielding Effectiveness of Metallic Enclosures with Apertures," *IEEE Trans. Electromagn. Compat.*, vol. 47, no. 3, pp. 456–462, 2005.

[14] S. Yenikaya and A. Akman, "Hybrid MoM/FEM Modeling of Loaded Enclosure with Aperture in EMC Problems," *Int. J. RF and Microwave CAE.*, vol. 19, pp. 204–210, 2009.

[15] M. P. Robinson, T. M. Benson, C. Christopoulos, J. F. Dawson, M. D. Ganley, A. C. Marvin, S. J. Porter, and D. W. P. Thomas, "Analytical Formulation for the Shielding Effectiveness of Enclosures with Apertures," *IEEE Trans. Electromagn. Compat.*, vol. 40, no. 3, pp. 240–247, 1998.

[16] T. Konefal, J. F. Dawson, A. Marvin, M. P. Robinson, and S. J. Porter, "A Fast Multiple Mode Intermediate Level Circuit Model for

the Prediction of Shielding Effectiveness of a Rectangular Box Containing a Rectangular Aperture," *IEEE Trans. Electromagn. Compat.*, vol. 47, no. 4, pp. 678–691, 2005.

[17] J. R. Mosig, "Scattering by Arbitrarily-Shaped Slots in Thick Conducting Screen: An Approximate Solution," *IEEE Trans. Antennas Propagat.*, vol. 52, no. 8, pp. 2109–2117, 2004.

[18] B. Q. Zhang, *Research on Mode-Matching Method in Microwave Passive Component Design*, Ph.D. Thesis, University of Electronic Science and Technology of China, 2004.

[19] G. Wu, X. G. Zhang, and B. Liu, "A Hybrid Method for Predicting the Shielding Effectiveness of Rectangular Metallic Enclosures with Thickness Apertures," *J. of Electromagn. Waves and Appl.*, vol. 24, no. 8–9, pp. 1157–1169, 2010.

[20] R. F. Harrington, *Time-Harmonic Electromagnetic Fields*, IEEE Press, 2001, 2nd edn.

[21] W. Wallyn , D. D. Zutter, and H. Rogire, "Prediction of the Shielding and Resonant Behavior of Multisection Enclosures Based on Magnetic Current Modeling," *IEEE Trans. Electromagn. Compat.*, vol. 44, no. 1, pp. 130–138, 2002.

[22] S. Celozzi, R. Araneo, and G. Lovat, *Electromagnetic Shielding*, Wiley-IEEE, New Jersey, 2008.

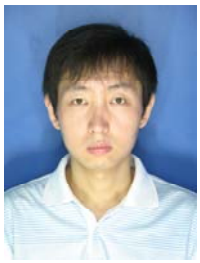

Gang Wu was born in Xi'an, Shaanxi, China, in 1981. He received his M.Sc. degree in Electronic Engineering from Xidian University, Xi'an, China in 2007. From 2008 to now, he is a doctor degree candidate in Xi'an division of China academy of space technology. His study direction is the theory and technology on electromagnetic protection.

Zhi-Qiang Song was born in Ya'an, Sichuang, China, in 1972. He received his M.S. degree in Electrical and Electronics Engineering from Xidian University, in 2005. He is currently working as a senior engineer at Xi'an division of China academy of space technology, Xi'an, China. His research interests are RF and microwave design, microwave measurements.

Xin-Gang Zhang was born in Shijiazhuang, Hebei, China, in 1980. He received his M.S. degree from Chongqing University, in 2007, in Electrical and Electronics Engineering. He is currently working as a doctor degree candidate at Xi'an division of China academy of space technology, Xi'an, China. His research interests are the theory of antenna, numerical studies of electromagnetic fields and waves.

Bo Liu was born in Changsha, Hunan, China, in 1962. He is currently working as a senior researcher at Xi'an division of China academy of space technology, Xi'an, China. His research interests are microwaves, radio wave propagation, and antennas.